

The Effect of Pressure on ZIF-8: Increasing Pore Size with Pressure and the Formation of a High-Pressure Phase at 1.47 GPa**

Stephen A. Moggach,* Thomas D. Bennett, and Anthony K. Cheetham

Recent interest in gas storage materials has led to a plethora of papers on the synthesis of novel metal–organic framework materials (MOFs).^[1–4] To date, structural variation in MOFs has been achieved through chemical modification, with accompanying changes in pore size and shape (and therefore internal surface area) giving rise to an increasingly diverse array of sorption properties. Such sorption measurements are performed at pressures up to 0.01 GPa; the effect of higher pressures on the framework is relatively unknown,^[5] though the mechanical stability of some MOFs at high temperatures have been discussed previously.^[6] The only structural data available as a function of pressure above 0.01 GPa on any MOF is on $[\text{Zn}(\text{C}_3\text{H}_3\text{N}_2)_2]$ (ZnIm),^[7] a dense zeolitic imidazolate framework (ZIF) material.^[8] ZIFs (a subfamily of MOFs), related to zeolites through the 145° angle subtended at the bridging imidazolate ligand, are of increasing interest. Their tuneable pore size, chemical robustness, and thermal stability combine the most desirable features of conventional MOF and zeolite structures, making them ideal candidates for gas storage applications.

In the study of ZnIm (which crystallizes in the tetragonal space group $I4cd$), the structure was found to undergo a phase transition at 0.8 GPa to a previously unknown phase (space group $I4_1$) involving a cooperative rearrangement of the framework, which was then recovered at ambient pressure. Although this material is a ZIF in terms of its topology, it contains no accessible pore volume. Herein we present the first high-pressure study on a porous ZIF, ZIF-8 ($\text{Zn}(\text{MeIm})_2$, MeIm = 2-methylimidazolate) with a sodalite zeolite-type structure and a large accessible pore volume (greater than 2000 \AA^3 per unit cell).

Prior to our pressure experiment, an X-ray data set was collected at ambient pressure and temperature on a crystal of ZIF-8 ($0.1 \times 0.2 \times 0.2 \text{ mm}$) to provide data for comparison with the high-pressure studies (which were also performed at

ambient temperature, see below). The same crystal was then loaded into a modified Merrill–Bassett diamond anvil cell (DAC) equipped with $600 \mu\text{m}$ culet diamonds and a tungsten gasket (Figure 1a).^[9] The sample and a chip of ruby (as a pressure calibrant) were loaded into the DAC with a 4:1 (v/v)

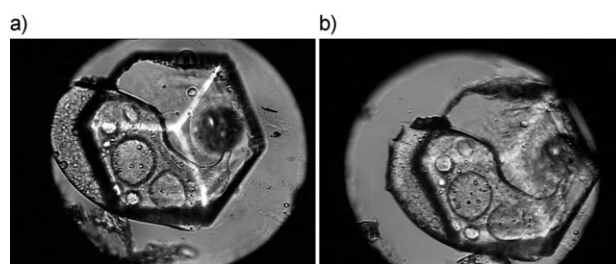


Figure 1. Optical images of a single crystal of ZIF-8 a) at ambient pressure and b) at 1.47 GPa (ZIF-8-II) in a diamond-anvil cell.

mixture of methanol and ethanol as a hydrostatic medium. The ruby fluorescence method was utilized to measure the pressure.^[10] High-pressure diffraction data were collected at 0.18, 0.52, 0.96, and 1.47 GPa. Data were also collected on decreasing pressure at 0.82 and 0.39 GPa. The sample was then downloaded from the pressure cell, and data was collected at ambient temperature and pressure after the pressure experiments. The pore volume and solvent content were calculated using the SQUEEZE algorithm within PLATON.^[11] Void analysis was carried out with the program MERCURY^[12] using a probe radius of 1.2 \AA and a grid spacing of 1.0 \AA .

ZIF-8 (phase I) crystallizes in the cubic space group $\bar{I}43m$ ($a = 16.9856(16) \text{ \AA}$, $V = 4900.5(8) \text{ \AA}^3$, Figure 2a). At ambient pressure and temperature, ZIF-8 contains one nanosized pore

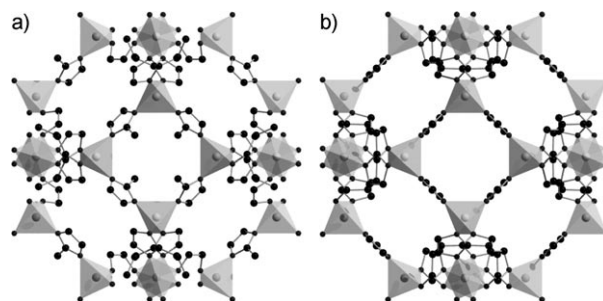


Figure 2. Packing arrangement of ZIF-8 a) at ambient pressure and b) at 1.47 GPa (ZIF-8-II). ZnN_4 tetrahedra are drawn as rigid polyhedra. H atoms are excluded for clarity. Note the change in orientation of the imidazolate groups on undergoing the transition from (a) to (b).

[*] Dr. S. A. Moggach
School of Chemistry and Centre for Science at Extreme Conditions
The University of Edinburgh
Kings Buildings, West Mains Road, Edinburgh, EH9 3JJ (UK)
Fax: (+44) 141-330-4888
E-mail: s.moggach@ed.ac.uk
Homepage: <http://www.chem.ed.ac.uk/staff/academic/moggach>
T. D. Bennett, Prof. A. K. Cheetham
Department of Materials Science and Metallurgy, University of Cambridge (UK)

[**] We thank the Royal Society of Edinburgh along with the Scottish government for a Personal Research Fellowship (to S.A.M.), and the EPSRC and ERC for funding (to T.D.B. and A.K.C., respectively).

Supporting information for this article is available on the WWW under <http://dx.doi.org/10.1002/ange.200902643>.

per unit cell; the pore is located at the center of the cell and has a volume of 2465 \AA^3 . Connecting these large nanopores are eight smaller channels (Figure 3a). From our ambient-

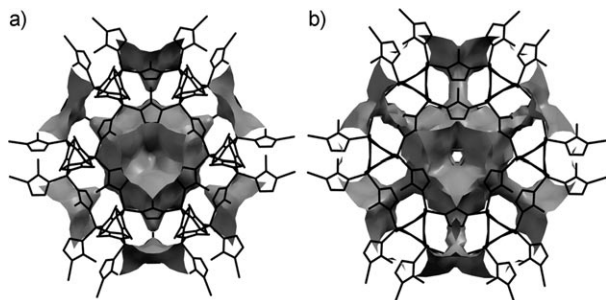


Figure 3. Void analysis, as carried out in the program MERCURY, of a) ZIF-8 at ambient pressure and b) ZIF-8-II at 1.47 GPa as viewed down the body diagonal. Note the increase in size of the funnels surrounding the central nanopore.

pressure single-crystal data, it was clear that some solvent was still in the pore. The electron count within the pore (calculated using the SQUEEZE algorithm within PLATON) measured $219 e^-$ per cell, corresponding to 12

Table 1: Crystallographic and pore data for ZIF-8 as a function of pressure.^[a]

Pressure [GPa]	<i>a</i> [Å]	Cell Volume [Å ³]	Total Pore Volume [Å ³]	Electron Count	MeOH Molecules
0	16.9856(16)	4900.5(8)	2465	219	12
0.18	17.0993(4)	4999.6(2)	2556	283	16
0.52	17.0630(4)	4967.8(2)	2529	381	21
0.96	16.9775(4)	4893.5(2)	2485	421	23
1.47 [#]	17.0710(17)	4974.8(9)	2439	636	41
0.82*	17.042(5)	4950(3)	2525	425	24
0.39*	17.093(5)	4994(3)	2541	337	19
0*	16.9920(8)	4906.1(4)	2447	41	2

[a] Phase II is indicated by [#] at 1.47 GPa. Pore volume, electron count, and number of MeOH molecules are calculated per unit cell. * refers to those values obtained on decreasing pressure.

molecules of methanol per unit cell (Table 1). On increasing pressure initially to 0.18 GPa, the sample actually increased in volume (from 4900.5(8) to 4999.6(2) \AA^3), with an associated increase in pore volume (2465 to 2556 \AA^3). This result is counterintuitive, as an increase in pressure usually results in a decrease in volume. Interestingly, the electron density within the pore also increased to $283 e^-$ per cell, thus indicating that the hydrostatic media surrounding the sample (used to apply pressure evenly) was being squeezed into the large nanopore, increasing the pore content and size as well as the cell volume. A broadly similar effect has been seen in zeolite- ρ ,^[13] though less dramatically than in the present case. On increasing the pressure further to 0.96 GPa, the cell and pore volume began to decrease, with the cell volume at 0.96 GPa remarkably being just below that measured at ambient pressure. The electron density within the pore,

however, continued to rise, measuring $421 e^-$ per cell at 0.96 GPa. On increasing the pressure further to 1.47 GPa, the sample underwent a single-crystal to single-crystal phase transition.

During the transition, the crystal appeared to jump in the pressure cell. This behavior can be seen in Figure 1 a, b, where the crystal has reoriented itself in a different location within the gasket chamber on undergoing the transition. There have been occasional reports of crystals that jump on undergoing phase transitions upon application of temperature (referred to as the thermosolvent effect); however, we could not find any reference to examples on application of pressure (barosolvent effect). Further study, however, is required to establish if a barosolvent transition truly occurs in this case.

The transition was also accompanied by a change in appearance of the crystal (note the rippled effect in Figure 1 b). The new high-pressure phase (ZIF-8-II) still maintains the $I43m$ space-group symmetry, but the imidazolate ligands twist, reorienting to increase the accessible pore volume (Figure 2). In particular, this reorientation increases the size of the eight narrow channels which link the nanopores throughout the framework (Figure 3). Although the volume of the nanopore decreases in size on undergoing the transition (from 2485 to 2439 \AA^3 at 0.96 and 1.47 GPa, respectively), the overall effect is to increase the pore volume owing to the increase in size of the linking channels. Remarkably, the cell volume increases on undergoing the transition and has a larger volume than that measured under ambient-pressure conditions. The total solvent in the pores at 1.47 GPa measures $738 e^-$ per cell, corresponding to 41 methanol molecules per unit cell, which is significantly higher than at ambient pressure (12 per unit cell). On decreasing the pressure, the transition was found to be reversible, and the crystal reverted back to phase I at 0.82 GPa. On removing the sample from the DAC, the cell volume reverted back to its ambient-pressure value; however, the pore volume and number of methanol molecules were found to be smaller than in same sample measured prior to the pressure experiment (Table 1).

Completely desolvating porous materials can often be difficult and may require heating the sample under high or low vacuum. In this case, by applying pressure we have removed the guest material from the compound, providing a new route by which to remove guest solvent from porous MOFs.

In summary, we have shown that by applying pressure to ZIF-8 we can force the hydrostatic medium to enter the pore, initially increasing the volume of both the nanopore and the unit cell. On increasing pressure further, more solvent can be forced into the nanopore, even though the nanopore volume decreases, until the sample undergoes a phase transition. This transition not only allows more solvent to enter the original nanopore, but it increases the size of the narrow channels that connect these pores, resulting in an overall increase in porous volume and amount of sequestered solvent. Modification of the pore volume, size, shape, and therefore selectivity has thus been achieved on application of pressure. Pressure could therefore be used as a means of inserting larger molecules into the pores which would otherwise be too small.

This approach could be used to increase the accessible surface area for gas storage materials. MOF-177, for example, has a pore large enough to include a C_{60} molecule, which may provide additional sites for sorption of H_2 or other gases.^[14]

The hydrostatic media that are used for pressure experiments are selected so as to apply pressure evenly to the sample. They are chosen on the basis of a number of factors, including the solubility and reactivity of the sample, but they also limit the highest pressures obtainable during the experiment (hydrostatic media become nonhydrostatic at elevated pressures and crush the sample). In this case, the hydrostatic medium (a 4:1 mixture of methanol and ethanol) interacts dynamically with the large accessible pore volume in ZIF-8. The compressibility of MOFs has been shown to depend on the hydrostatic medium;^[15] however, this is the first detailed example showing what happens to the structure of a porous MOF on increasing pressure. Effects include an unprecedented increase in volume on increasing pressure, a pressure-induced phase transition (modifying the pore size, shape, and volume), and an unexpected removal of guest solvent molecules from the framework, without structural degradation.

Experimental Section

A solid mixture of zinc(II) nitrate hexahydrate (0.525 g, 1.76×10^{-4} mol) and 2-methylimidazole (MeIM; 0.015 g, 1.83×10^{-4} mol) was dissolved in DMF (9 mL) in a 12 mL Teflon-capped vial. The vial was heated at a rate of 200°C h^{-1} to 130°C , held at this temperature for 24 h, and then cooled at a rate of 5°C h^{-1} to room temperature. Colorless polyhedral crystals were filtered from the reaction mixture, washed with chloroform (3×5 mL), and dried in air (30 min). Yield: 0.0064 g, 11 % based on 2-methylimidazole. The product was formulated using elemental analysis as $Zn(\text{MeIM})_2(\text{DMF})(\text{H}_2\text{O})$ ($C_{11}H_{19}N_5O_2Zn$). Calcd C 41.51, H 5.97, N 22.01; found: C 42.04, H 5.46, N 21.83. The sample was immersed in methanol for 48 h at ambient temperature to effect solvent exchange, which was confirmed by thermogravimetric analysis and IR spectroscopy.

X-ray diffraction data were collected with $\text{MoK}\alpha$ radiation ($\lambda = 0.71073 \text{ \AA}$) at room temperature and pressure on a Bruker Smart Apex diffractometer. Refinement was carried out against $|F|^2$ in CRYSTALS^[16] starting from the low-temperature coordinates of Wu et al.^[17] High-pressure diffraction data were collected on the same sample ($0.2 \times 0.2 \times 0.1 \text{ mm}^3$) on a Bruker APEX II diffractometer with graphite-monochromated $\text{MoK}\alpha$ radiation ($\lambda = 0.71073 \text{ \AA}$). Data were collected in ω -scans in twelve settings of 2θ and ϕ with a frame and step size of 40° and 0.3° , respectively. This data collection strategy was based on that described by Dawson et al.^[18] The data were integrated using the program SAINT^[19] using dynamic masks to avoid integration of regions of the detector shaded by the body of the pressure cell.^[18] Absorption corrections for the DAC and sample were carried out with the programs SHADE^[20] and SADABS,^[21] respectively. High-pressure refinements of ZIF-8 were carried out against $|F|^2$ using the program CRYSTALS.^[16] All 1,2- and 1,3-distances of the 2-methylimidazolate ligand were restrained to the values observed in our ambient-pressure structure. All torsion angles and metal-to-ligand distances were refined freely. Hydrogen atoms attached to carbon were placed geometrically on the basis of the neutron data from reference [17].

The structure of phase II at 1.47 GPa was solved by SIR92.^[22] The numbering scheme used is the same as CSD refcode OFERUN. Data

from the downloaded sample (after the pressure experiment) were collected at room temperature. The same experimental procedure was carried out as for the room-temperature collection described above. Detailed crystallographic data are summarized in the Supporting Information. CCDC 739161 (0 GPa), 739162 (0.18 GPa), 739163 (0.52 GPa), 739164 (0.96 GPa), 739165 (1.47 GPa), 739166 (0.82 GPa), 739167 (0.39 GPa), 739168 (0 GPa) contain the supplementary crystallographic data for this paper. These data can be obtained free of charge from The Cambridge Crystallographic Data Centre via www.ccdc.cam.ac.uk/data_request/cif.

Received: May 18, 2009

Published online: August 13, 2009

Keywords: crystal engineering · high-pressure chemistry · organic–inorganic hybrid composites · polymorphism

- [1] R. Banerjee, A. Phan, B. Wang, C. Knobler, H. Furukawa, M. O’Keeffe, O. M. Yaghi, *Science* **2008**, *319*, 939.
- [2] R. Kitaura, G. Onoyama, H. Sakamoto, R. Matsuda, S.-i. Noro, S. Kitagawa, *Angew. Chem.* **2004**, *116*, 2738; *Angew. Chem. Int. Ed.* **2004**, *43*, 2684.
- [3] A. K. Cheetham, C. N. R. Rao, R. K. Feller, *Chem. Commun.* **2006**, 4780.
- [4] G. Férey, *Chem. Soc. Rev.* **2008**, *37*, 191.
- [5] S. A. Moggach, S. Parsons, *Spectrosc. Prop. Inorg. Organomet. Compd.* **2009**, *40*, 324.
- [6] J. Hafizovic Cavka, S. Jakobsen, U. Olsbye, N. Guillou, C. Lamberti, S. Bordiga, K. P. Lillerud, *J. Am. Chem. Soc.* **2008**, *130*, 13850.
- [7] E. C. Spencer, R. J. Angel, N. L. Ross, B. E. Hanson, J. A. K. Howard, *J. Am. Chem. Soc.* **2009**, *131*, 4022.
- [8] R. Lehnert, F. Seel, *Z. Anorg. Allg. Chem.* **1980**, *464*, 187.
- [9] S. A. Moggach, D. R. Allan, S. Parsons, J. E. Warren, *J. Appl. Crystallogr.* **2008**, *41*, 249.
- [10] G. J. Piermarini, S. Block, J. D. Barnett, R. A. Forman, *J. Appl. Phys.* **1975**, *46*, 2774.
- [11] A. L. Spek, Utrecht University, Utrecht, The Netherlands, **2004**.
- [12] I. J. Bruno, J. C. Cole, P. R. Edgington, M. Kessler, C. F. Macrae, P. McCabe, J. Pearson, R. Taylor, *Acta Crystallogr. Sect. B* **2002**, *58*, 389.
- [13] Y. Lee, J. A. Hriljac, T. Vogt, J. B. Parise, M. J. Edmondson, P. A. Anderson, D. R. Corbin, T. Nagai, *J. Am. Chem. Soc.* **2001**, *123*, 8418.
- [14] J. L. C. Rowsell, O. M. Yaghi, *Angew. Chem.* **2005**, *117*, 4748; *Angew. Chem. Int. Ed.* **2005**, *44*, 4670.
- [15] K. W. Chapman, G. J. Halder, P. J. Chupas, *J. Am. Chem. Soc.* **2008**, *130*, 10524.
- [16] P. W. Betteridge, J. R. Carruthers, R. I. Cooper, K. Prout, D. J. Watkin, *J. Appl. Crystallogr.* **2003**, *36*, 1487.
- [17] H. Wu, W. Zhou, T. Yildirim, *J. Am. Chem. Soc.* **2007**, *129*, 5314.
- [18] A. Dawson, D. R. Allan, S. Parsons, M. Ruf, *J. Appl. Crystallogr.* **2004**, *37*, 410.
- [19] Bruker-Nonius, Bruker-AXS, Madison, Wisconsin, USA, **2006**.
- [20] S. Parsons, The University of Edinburgh, Edinburgh, United Kingdom, **2004**.
- [21] G. M. Sheldrick, Bruker-AXS, Madison, Wisconsin, USA, **2004**.
- [22] M. C. Burla, R. Calandro, M. Camalli, B. Carrozzini, G. L. Cascarano, L. De Caro, C. Giacovazzo, G. Polidori, R. Spagna, *J. Appl. Crystallogr.* **2005**, *38*, 381.